

How to Cite:

Sultan, A. A. H. (2022). The effectiveness of nano-cobalt oxide with manufactured plant extract and its properties on inhibiting the growth of some types of bacteria and fungi isolated from skin infections. *International Journal of Health Sciences*, 6(S9), 1878–1893.
<https://doi.org/10.53730/ijhs.v6nS9.12829>

The effectiveness of nano-cobalt oxide with manufactured plant extract and its properties on inhibiting the growth of some types of bacteria and fungi isolated from skin infections

Asmaa Ahmed Hatem Sultan

Technical Medical Institute, Middle Technical University, Baghdad, Iraq.
Corresponding author email: assma2222@mtu.edu.iq

Abstract---The prepared cobalt oxide nanoparticles were manufactured in the first and second methods, and they show the properties of the nanomaterials for all solutions of plant extracts. XRD examination showed (440) 65, (622) 79, while Sem's examination showed the appearance with a size of 10-25 nm. Tem examination gave that nanoparticles with a size not exceeding 0.5-60 nm. The UV absorbance and permeability test indicated that the nanomaterial is at a value between 236-800nm, and energy gap values of 2.0-3.8 ev. Ft-ir assay shows that the bonding sites for cobalt oxide are at (± 50) (505 to 694), and the Zeta Potential test indicated that all the particles of the solutions have very small values and that the material is not agglomerating. The Aleo vera plant extract with cobalt oxide nanomaterial, where the diameters of the inhibition zones were (35, 35, 45) mm, respectively, for the growth of both *Ps.aeruginosa*, *S. aureus* and *E.coli* bacteria. The results of the effect of cobalt oxide solutions on the inhibition of the growth of fungi were great, and that the nanomaterial was also sweeping, showing the absence of fungal growth *Trichophyton mentagrophytes*. However, the effect of the nanomaterial prepared by the second method was more inhibiting (30,33,33 mm compared to the solutions prepared by the first method (22,15,12) mm in inhibiting the fungal growth of *Candida albicans*.

Keywords---Aleo vera, XRD, SEM, TEM, UV, FRIT, ZETA POTENTIAL, *Ps.aeruginosa*, *S. aureus*, *E.coli*, *Trichophyton mentagrophytes*, *Candida albicans*, CoO, Green synthesis nanoparticles by plant extract, artificial roads nanoparticles.

Introduction

Nanotechnology is the term used to cover the design, construction and functional use of structures with at least one distinct dimension measured in nanometers (Pal, Jana, Manna, Mohanta, & Manavalan, 2011). The physical (top-to-bottom) and chemical (bottom-up) approaches are usually expensive and costly processes, not environmentally friendly and have toxic effects (Honary, Barabadi, Gharaei-Fathabad, & Naghibi, 2012). Modern methods have been introduced to the fabrication made of high-quality nanomaterials. This can be achieved by a simple green synthesis compared to conventional micro-synthetic nanoparticles. It would help to eliminate difficult processing conditions, by allowing synthesis at physiological pH, temperature, pressure and low cost (Bardaji et al., 2016).

The skin is the first mechanical barrier that prevents pathogens and foreign materials from penetrating it and causing infection (Cianci, Slade Jr, Sato, & Faulkner, 2013). *S. aureus* is a Gram-positive bacterium. It has a spherical shape and a diameter of 1.0-0.7 microns. It appears under the microscope in irregular clusters and may appear singly or in the form of a short assembled chain that is non-motile and does not form spores (Al-Nashi & Al-Mansoori). It is one of the most important species from a medical point of view and it can be distinguished from the rest of the other species by its ability to produce the plasma clotting enzyme, which is one of the main virulence factors in these bacteria (Al-Salmi, 2014). *Ps. aeruginosa*, a Gram-negative bacterium with dimensions of about 0.6 x 2 microns, is not sporangia-forming, transmitted by a polar flagellum that forms a living antenna. It is an opportunistic pathogen that causes 10-20% of hospital infections. This bacterium is considered one of the very dangerous bacterial species because the infections caused by it are difficult to treat because it is one of the species that is characterized by its multi-resistance to life antibiotics (Al-Hilli, 2000). It becomes a strong pathogen whenever it enters the areas devoid of defenses, as in the case of skin and mucous membrane ruptures, helped by their possession of a number of various virulence factors, such as the production of hemolytic enzymes (Haemolysin), proteinase and the production of many exotoxins that are equivalent in effectiveness to Diphtheria toxin (Behzadi, Baráth, & Gajdács, 2021). This bacterium is the most common cause of burn injuries (Bassetti, Vena, Croxatto, Righi, & Guery, 2018), and it was found that about 25% of burn patients hospitalized for treatment are infected with this bacterium. *E. coli* 6-5×1.5- Microns arranged singly or in pairs, moving by circumferential flagella, are immobile and consumed most carbohydrates, forming acid with gas, and their colonies appear dry and pink on the medium of the MacConkey for fermentation of lactose sugar. Two types of exotoxins are produced: the first is heat labile, and the other is heat stable, and causes cases of summer diarrhea in infants. It also causes infections of wounds and burns as a result of its movement from its natural place of existence, which is the intestines,

to other areas of the body, in addition to being considered the first pathogen that it infects the urinary tract, causing urinary tract infections of varying severity.

Dermatophyte *T. mentayrophyte* is characterized by flat, domed, white colonies with copious conidia and the edges of the colonies are semi-radial. Small conidia often appear in clusters and arranged on the sides of the hyphae (Ernest Jawetz, Adelberg, & Melnick, 1987). This fungus is the main cause of tinea pedis (*Tinea pedis*) as well as body tinea. This type is the main cause of tinea capitis, tinea auris, tinea auris, and tinea manum (Alteras, Aryeli, & Feuerman, 1980). As for *Candida albicans*, it is the most common type that infects the skin in different areas of the human body. Its cells are characterized by their oval shape, and their diameters range between 10-6 x 6-3.5 microns. It is in the form of single cells or in the form of pseudophypha in the tissues of the host as it forms the germ tube, which is the preparatory stage for the invasion of host tissues (Soll & Beddl 1978). The external parts of the body, such as the skin, hair and nails, are exposed to infection with this yeast because they possess two types of enzymes, which are proteinase and keratinase, which help them to infect the outer layer of the keratinized (Negi, Tsuboi, Matsui, & Ogawa, 1984). In the armpit, under the breasts and between the fingers, the infection occurs in the form of vesicles, then turns into dark red spots accompanied by itching and burning with crusting in the area (E Jawetz & Melnick, 1980).

Materials and Methods

Preparation of cobalt oxide in two ways: The first method is nanoparticle structure

A - 1M molar sodium hydroxide NaOH is prepared from 4 g of sodium hydroxide and dissolve 100 ml of distilled water (Aesar, 2011).

B- A solution of cobalt nitrate ($\text{Co}(\text{NO}_3)_2$) is prepared with a molecular weight of 183.32 to prepare a molarity that is equal to, $M = \text{weight} / \text{molecular weight} \times 1000 / \text{required volume}$. The weights are $M = \text{weight} \setminus 236.42 \times 1000 \setminus 100$, $M = 18.6$ g. A weight of 18.5 g of cobalt nitrate was dissolved directly in 100 ml and transferred to a magnetic stirrer for an hour at a temperature of 30-70 ° C with spiral motion using a magnetic pole inside solution until it melts and the color stabilizes for an hour or more. The two solutions are mixed by adding solution A to solution B gradually and then left for an hour at a temperature of 30-70 C with spiral motion using a magnetic pole inside the solution until it dissolves. Then a sample of the solution is taken in a test tube to compare the color until the color stabilizes for an hour or more. It is the salt formed. Tests are conducted on the formation of nickel oxide for the nanocomposite after its preparation (Saad & Karim, 2017).

Preparation of nano-solutions: Cobalt oxide, CoO, method 2 green nanpractical

A- Preparing aloe vera solution(Patnaik, 2003)

A weight of 10 g of *aloe vera* pulp is taken and 100 ml of distilled water is dissolved and placed on a magnetic stirrer for an hour at a temperature of 30-70 ° C with a spiral motion using a magnetic pole inside the solution until it dissolves. It is then filtered using cotton inside a glass funnel and repeated again After completing the volume with water to 100 ml and transferred to a magnetic stirrer until the color stabilizes for an hour or more, depending on the solution, by following the sediment until it disappears and the color is stable.

B- Preparing of a solution of cobalt nitrate (Co(NO₃)₂) with a molecular weight of 183.32 to prepare a molarity

$M = \text{weight} / \text{molecular weight} \times 1000 / \text{desired volume}$, $M = \text{weight} / 236.42 \times 1000 / 100$ $M = 18.5$ g. 18.5 g of cobalt nitrate was taken, dissolved directly in 100 ml, transferred to a magnetic stirrer for an hour at a temperature of 30-70 ° C with spiral motion using a magnetic electrode inside the solution until it dissolved. Then, a sample of the solution was taken in a test tube to compare the color until the color stabilized for a period of an hour or more, depending on the solution, by following the sediment until it disappears and the color is stable. The two solutions are mixed by adding solution A to solution B gradually. It is then left for an hour at a temperature of 30-70 C with spiral movement using a magnetic pole inside the solution until the color stabilizes for an hour or more according to the solution by following the precipitate until it disappears and color stability.



A



B



A. Preparing cobalt nitrate and mix it with a solution of *aloe vera* to obtain a solution of cobalt nitrate with Aloe vera

B A solution of cobalt nitrate with a solution of cobalt hydroxide is prepared. It is mixed and appears thick, cobalt oxide salt.

Bacterial Pathogen Isolates

The swab was taken with a sterile swab (Swab) and transferred to the hospital laboratory and initially cultured on blood agar medium in MacConkey agar medium.

Also, EMB agar was incubated at 37°C for 48-24 hours. The bacteria were identified morphologically, bacteriologically and biochemically.

Preparation of culture media for Fungal Pathogen Isolates

Isolation and Identification of Fungi and pathogenic yeast:

Fungi and yeasts were diagnosed and isolated based on the phenotypic characteristics of the colony, such as the shape, color, diameter, and height of the colony, as well as the microscopic characteristics such as the shape, size and color of conidia. In addition, some chemical tests were adopted in the diagnosis using the following sources (Feliciano Guzmán, 2016). Culture of Specimens are as follows: after direct microscopic examination of the samples, a portion of the sample was taken and planted on the surface of a sterile glass dish containing SDA Sabouroud Dextrose Agar Medium to prevent the growth of bacteria and sauropod fungi (non-pathogenic) and thymine and yeast extract were added to SDA to promote the growth of some types of filamentous dermatophytes and incubated. Cultures were conducted at 28-30°C for filamentous fungi and at 37°C for yeasts. Sabouroud Dextrose Agar Medium (SDA) was prepared according to Emmons (1974) by dissolving 40 gm of dextrose, 10 gm of peptone, 20 gm of agar and 0.05 gm of the antibiotic chloramphenicol, then completing the volume to 1000 ml using distilled water and placing the mixture in clean and sterilized glass flask in a sterilizer at a temperature of 121°C and a pressure of 15 pounds / in² for 20 minutes. After sterilization, chlorine was added. This medium was used before to isolate opportunistic fungi (Al-Mousawi, 1997).

Emmons sabouroud Dextrose Agar Medium (ESDA) was prepared according to what was reported in (McGinnis, 1980) by dissolving 20 gm dextrose, 10 gm peptone, 20 gm agar and 0.05 gm of the antibiotic Chloramphenicol. It was added after sterilization and then the volume was completed to 1000 ml of distilled water and then sterilize the medium with autoclave at a temperature of 121 °C and a pressure of 15 pounds / in² for a period of 20 minutes. Germ tube test was carried out according to Collee, Fraser, Marmion, and Simmons (1996) to differentiate between the species belonging to the genus *Candida* Spp. This is done by inoculating 0.5 ml of sheep serum with inoculum from colonies of this genus and incubated at 37 °C for 2-3 hours. The formation of the germ tube is an indication of the positive test, and this test is a characteristic of *C. albicans*. The emergence of the germ tube from one side of the cell is observed when part of the colonies is incubated with sheep serum for 2-3 hours at a temperature of 37 °C.

Discussions and Findings

Examinations of the cobalt oxide nanomaterial: XRD examination is a test of cobalt oxide formation by matching the results with international standards and corresponding graphs (Jalil, Raghad, Nuaman, & Abd, 2016).

Table 1
values the Miller's treatment (MT) coefficient for cobalt oxide by
matching the results with international standards and the
corresponding graphs

Miller's treatment value)MT(CoO	international standards	2 theta (deg) NT1(2 Theta (deg)(NT2
111)(CoO	19	19.2	19.1
220)(CoO	31	31.55	31.4
311)(CoO	38		
CoO(400)	45	45.1	45
511)(CoO	59	59.65	59.55
(440) CoO	65	65.55	65.4
622)(CoO	79	79	79

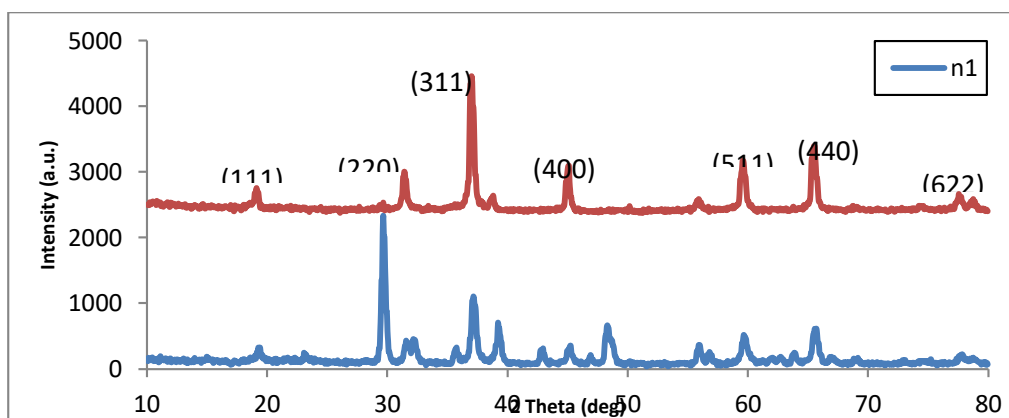


Figure 1. Diagram of XRD examination of the cobalt oxide solution NT1, the first method, in comparison with the extract NT2 for the cobalt oxide, the second method

It is evident from Table (1) that the results of the examination are close to the international measurements of Miller's treatment coefficient and indicate the presence of cobalt oxide in the samples of the first and second methods. Through the graph of the cobalt, graph No. (1) shows the presence of nanomaterials 19 (111, 31 220)), 45 (400), 59 (511), 65 (440), 79 (622) in each of NT1. The results are consistent with the graph of the first and the second method with the international measurements of Miller's coefficient and Theta 2 (deg). SEM assay: It is a test of morphological properties to find the size and shape of the nanoparticle during sedimentation.

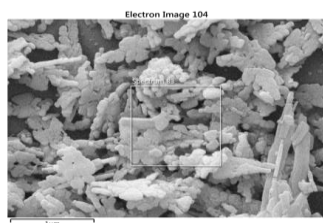


Figure 2. The SEM results of the sample NT1

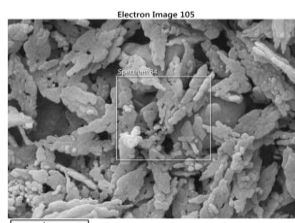


Figure 3. The SEM results for the sample NT2

Figure No. (2) is NT1 material that is deposited on the glass, where the black background shows the shapes of rock or cork particles, almost spherical and semi-spherical shapes with dimensions not exceeding 200 nm at the drawing scale. These particles appear with dimensions of drawing size 25 nm smaller than 100 nm. Figure No. (3) NT2 shows the spherical or semi-spherical particle and the rest of the aggregates, such as limestone sedimentary rocks, the smallest size of 10 nm, and they may aggregate to a size of up to 300 nm for nanoparticles. TEM assay: It is a test to find the shape and size of a nanoparticle particle prior to deposition..

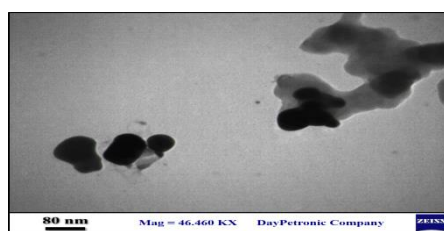
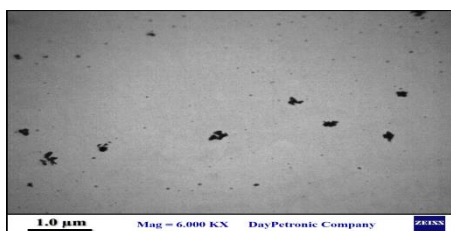


Figure 4. TEM Cobalt Oxide NT1 Solution First Method

Figure No. (4) shows NT1 that nanoparticles in the solution, the largest image scale A was 3.5 μm. They are spherical bodies connected to each other, and according to the scale in the image B, the scale of the nanoparticle does not exceed 60nm.

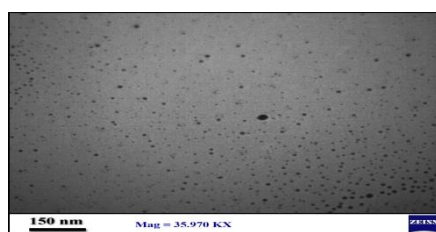
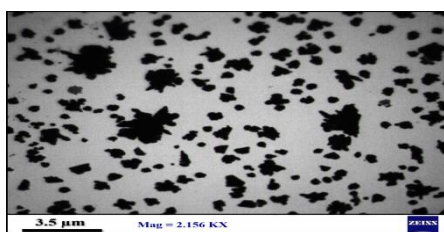


Figure 5. TEM Cobalt oxide solution NT2 Second method

Figure No. (5) NT2 that nanoparticles in the solution are largest scale of image A (3.5 μm). It is single and large spherical bodies connected to each other. The scale in Image B shows nanoparticles whose drawing scale was 150 nm.

UV test is the test of transmittance and absorption coefficient and determines the energy gap.

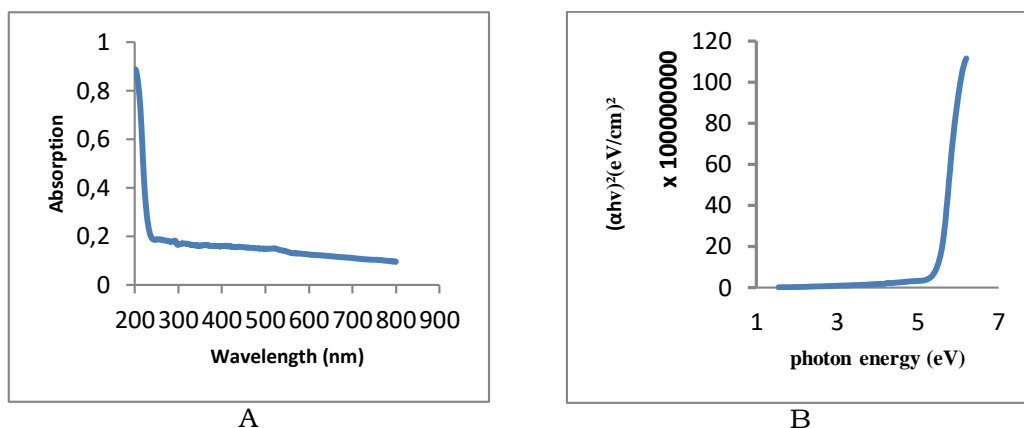


Figure 6. UV, energy and absorption gap of NT1 cobalt oxide solution First method

Figure No. (6) is a UV graph A. It is the absorbance of NT1 cobalt oxide solution, of the first method deposited on glass. It is noted that the material has a high absorbance at 200 - 236 nm, and that at more than 236 nm it has very little absorbency (high transmittance), which is the range from 236 - 800 nm. Also, the material with high permeability behaves like a window (it is an optical property that means the material transparent in the visual sense). Here, transparent means that the solution is homogeneous and very light very well. This is due to the complete homogeneity of the material and the deviation of absorption towards short waves, which indicates the formation of very small nanoparticles. Figure (6), is UV diagram B is the energy gap, which is important in electronic transitions, and it is an optical property. The importance of the energy gap is that the curve is in contact with the x-axis and cuts it by a point. This point is an angle called the energy gap is 3.5 eV. It is a semiconductor material and it achieves the oxide of the nanomaterials.

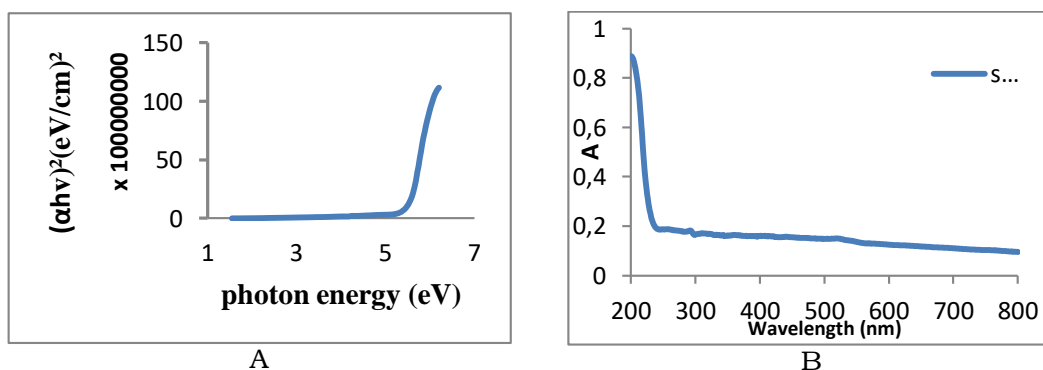


Figure 7. UV Absorption and Energy Gap Cobalt Oxide NT2 Solution Second Method

Figure No. (7) shows UV absorbance and energy gap, cobalt oxide solution and NT2 of the second method. Diagram A indicates that the material is transparent with high permeability and very little absorption at the range 236-800nm. This is evidence that the solution is homogeneous and light very well. This is due to the complete homogeneity of the material and its deflection of absorption towards short waves indicates the formation of very small nanoparticles. Graph B is the energy gap with a high value is 3.8 eV, which is a semiconductor material that achieves the oxide of the nanomaterials.

FT-ir Test: It is a test to check and identify effective chemical bonds

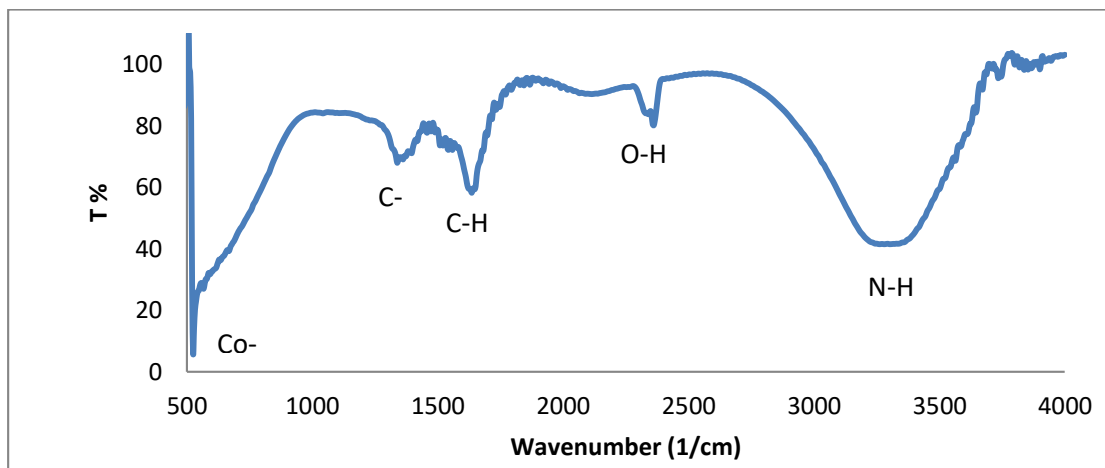


Figure 8. is FT-IR cobalt oxide solution NT1 of the first method This figure shows FT-IR cobalt oxide solution NT1. The first method is the bond locations of metal oxide Co-O at (± 505) (50 to 694) and it is present, but the wavelength of 1315 is at the C-N bond level. It may be 1300 CN bonds, 2400 OH bonds, 3251 NH bonds, and these are according to the vibration table in the source. (Enders, A., 2021).

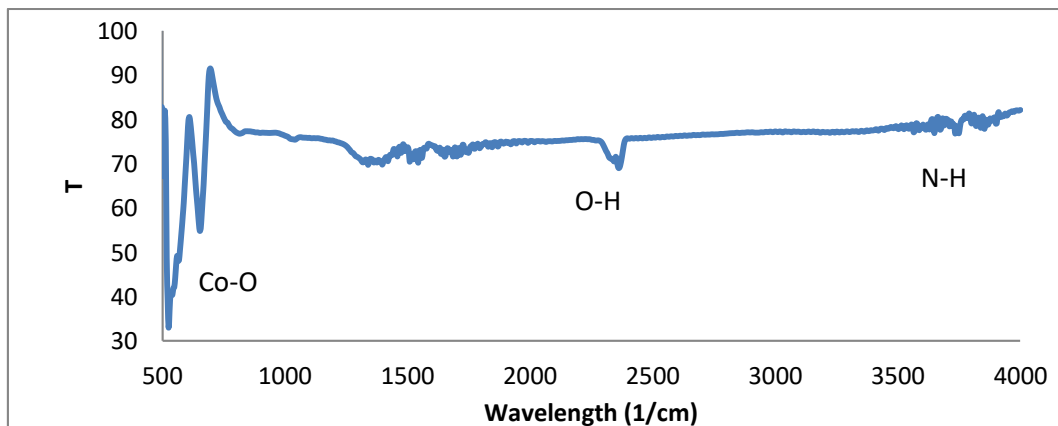
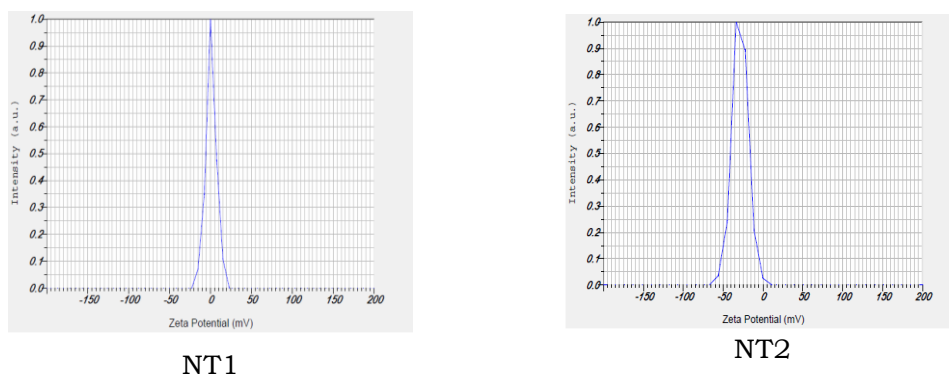


Figure 9. FT-IR cobalt oxide solution NT2 of the second method.

Figure No. (9) is FT-IR cobalt oxide solution NT2 of the second method. The locations of the metal oxide Co-O bonds are at (± 505) (50 to 694). Here, the wavelength of 1315 is at the C-N bond level, it may be 2400 OH bonds, 3500 NH bonds, and this is according to the vibration table of the source(Enders, North, Fensore, Velez-Alvarez, & Allen, 2021). The presence of an NH bond is an amino acid bond for a type of proteins. Also, the importance of effective bonds maintains the dimensions between the materials and maintains the sizes and does not occur agglomeration. The presence of NH confirms its presence on t of the plant substance in the solution as the presence of bonds C, O, H is an evidence of metal oxide minerals and lack of acidic materials. The presence of the plant is important in the process of oxidation, reduction and color transformation in the solution. It has a great role in encapsulating nanoparticles in order not to cause an agglomeration process of the material. Whenever the nanomaterial decreases, the particles with a strong charge, high attraction and repulsion do not agglomerate. Also, the material does not settle at the bottom of the pot(Abdel-Aal, Beskrovnyi, Ionov, Mozhchil, & Abdel-Rahman, 2021). ZETA Assay is the determination of particle size and surface charge of dynamic light scattering zp factor potentials(Instruments, 2012).



Peak No.	Zeta Potential	Electrophoretic Mobility
NT1	0.9 mv	0.000007 cm ² / vs
NT2	-28.5 mv	-0.000221 cm ² /vs

Figure 10. The results of Zeta Potential for cobalt oxide solutions, the first method NT1 and the second method NT2.

The results of the Zeta examination show a positive dissonant value, which is the evidence of positive charges. As for the negative values are the presence of negative discordant charges. The solutions of No. (NT1, NT2) are the nano-solutions prepared in the first and in the second methods. The value of the graph Zeta Potential is a figure. (10) are, respectively (0.9 mv, -28.5 mv). It is noted that the values of mv are negative and very few, which means that no agglomeration occurs in the nanomaterial.

Effect Of Nanosolutions on Bacterial Growth

From Table No. (2) and Figure No. (11), it is noted that the extract of *Aloe vera* plant with cobalt chloride had its effect on inhibiting the growth of pathogenic bacteria, *E.coli*, *Ps.aeruginosa*, *S. aureus*, and at the rates of diameters of inhibition. These rates of the diameters of the inhibition zone were (, 35, 35,45 (35,37,4735,37,47) mm) respectively, as it turns out that the solution of the second method NT2 was more effective in resisting the two types of bacteria and in approximately equal proportions. (14,11,14) mm less effect compared to the second method. This proves that the materials contained in *Aleo vera* plant synergistically with the nano-material in affecting bacteria and making them more effective(Li et al., 2012). The effect of the solution of the second method on *S. aureus* was more bacteria at low concentrations than at high concentrations because the nano-materials are more effective at low concentrations than at high concentrations because the solution is more dilute and the material does not agglomerate and gives more effect(Jirátová et al., 2019). The same effect is noted on inhibiting the growth of bacteria *E. coli*. The extracts of the first method had less effect of cobalt oxide in all high concentrations on *Ps. aeruginosa*-negative bacteria. The reason for this may be due to the nature of the bacterial cell wall, as Gram-negative bacteria contain a layer of the outer membrane that makes its permeability to materials less compared to the positive bacteria in terms of response(Sokrab, 2010). Here, the inhibition of the growth of *S.aureus* bacteria with the solutions prepared in the first method was more effective than the inhibition of the growth of *Ps. aeruginosa* bacteria and this is consistent with what was found(Maruthamuthu & Ramanathan, 2016). Yet, the nano plant extracts at a concentration of 25%M did not inhibit bacterial growth at rates (0.0%), as the bacteria were resistant to this concentration for each of the bacteria *Ps.aeruginosa*, *S.aureus*, and *E.coli*(Ahmed, Aly, Abd El-Baky, & Waly, 2020; Behzadi, Baráth, & Gajdács, 2021).

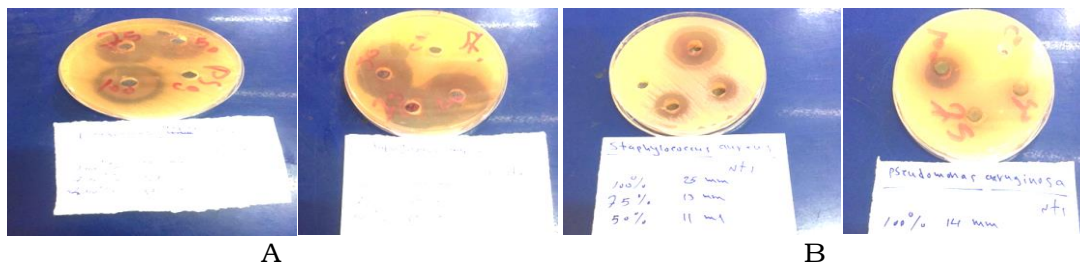


Figure (11) shows the areas of inhibition on culture media using NT2 extract of the second method for some types of bacteria, while B shows the effect of solutions of the first method NT1 and measured | - | mm The numbers refer to the concentrations used. 20mm=1cm
 S = *S. aureus* , Ps = *Ps. aeruginosa* 1 =100 M , 2 =75 M
 3 = 50 M, 4 = C = Control.

Table 2
Shows the effect of nano-solutions prepared in the first and second methods on inhibiting bacterial growth

Method name	concentration	Average length of inhibition area mm	Average length of inhibition area mm	Average length of inhibition area mm
Bacteria name	%	<i>Ps.aeruginosa</i>	<i>S.aureus</i>	E. coli
1 NT1	25	0.0	0.0	0.0
	50	0.0	25	0.0
	75	0.0	13	0.0
	100	14	11	14
2 NT2 Aleo vera	25	0.0	0.0	0.0
	50	35	35	35
	75	37	35	37
	100	47	45	47

NT1: cobalt nitrate + sodium hydroxide, NT2: cobalt nitrate + aloe vera.

The effect of cobalt oxide on fungal growth

Table 3
Shows the percentage of nanoparticle concentration in the first and second method and its effect on fungal growth

Method	concentration %	The length of the diameter of the inhibition area mm	The length of the diameter of the inhibition area mm
		<i>Candida albicans</i>	<i>Trichophyton mentagrophytes</i>
1	0.0	0.0	0.0
	50	12	There is no fungal growth
	75	15	There is no fungal growth
	100	22	There is no fungal growth
2 Aleo vera	0.0	0.0	0.0
	50	33	There is no fungal growth
	75	33	There is no fungal growth
	100	45	There is no fungal growth

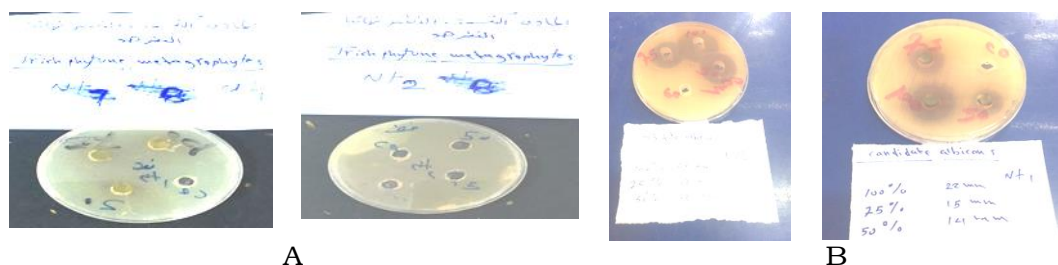


Figure 11. A shows the results were sweeping the absence of fungal growth *Trichophyton mentagrophytes* while B is the effect of nanomaterials on the inhibition of fungal growth *Candida albicans*.

Table No. (3) and Figure No. (11) explain that the results of the effect of cobalt oxide solutions on inhibiting the growth of fungi were significant, and that the nano-material was sweeping, showing the absence of fungal growth, *Trichophyton mentagrophytes*, In terms of *Candida albicans*, the effect of the nanomaterial prepared by the second method was more inhibiting (30,33,33 mm, respectively) compared with the solutions prepared by the first method (12,15,22 mm), respectively, to inhibit the fungal growth of *Candida albicans*.

Conclusions

The growth inhibition activity of the plant extract with the cobalt oxide nanoparticle prepared by the second method, Green synthesis nanoparticles by plant extract, is more efficient than the nanoparticle prepared by the first method, artificial roads nanoparticle, in inhibiting the growth of isolates of *S.aureus* *E.coli*, *Ps.aeruginosa*. Also, it was effective in inhibiting growth significantly and scavenging the fungi *Trichophyton mentagrophytes*, *Candida albicans*.

Recommendations

This work recommends the following:

- 1- Conducting chemical and technical studies of the active chemical components of nanomaterials for use in medical and therapeutic purposes.
- 2- Using the GCMS examination of solutions to test the chemical content and applying a study of the possibility of using these extracts against pathogens in vivo In vivo, especially for other non-dermatological therapeutic uses of these extracts.

References

- A Abdel-Aal, S. K., Beskrovnyi, A. I., Ionov, A. M., Mozhchil, R. N., & Abdel-Rahman, A. S. (2021). structure investigation by neutron diffraction and x-ray diffraction of graphene nanocomposite CuO-rGO prepared by low-cost method. *physica status solidi (a)*, 218(12), 2100138.

- Aesar, A. (2011). Bisphenol A MSDS No. A10324; Alfa Aesar, A Johnson Matthey Company: Ward Hill, MA. In.
- Ahmed, F. Y., Aly, U. F., Abd El-Baky, R. M., & Waly, N. G. (2020). Comparative study of antibacterial effects of titanium dioxide nanoparticles alone and in combination with antibiotics on mdr pseudomonas aeruginosa strains. *International Journal of Nanomedicine*, 15, 3393.
- AL-Hilli, F. (2000). Study of Antimicrobial effect of leaves extract from Callistemoncitrinuson Pseudomonas aeruginosa isolated from patients. M. Sc. Thesis, Coll. Sci., Univ. AL-Mustansiriya,
- Al-Mousawi, A. A.-K. (1997). Presence of opportunistic pathogenic keratinocytes in the dust of the floor of some hotels and mosques in Basra Governorate. (Master Unpublished). University of Basra, College of Science.
- Al-Nashi, A. A.-R., & Al-Mansoori, R. W. H. Investigation of the phenotypic and molecular pattern of virulence factors of Staphylococcus bacteria. Staphylococcus spp, hemolyzed and isolated from urinary tract infections in Al-Diwaniyah. College of Education - University of Al-Qadisiyah: Department of Life Sciences.
- Al-Salmi, B. T. S. (2014). The Study of some factors in the production of coagulase from locally isolated Staphylococci. (Master). University of Karbala,
- Alteras, I., Aryeli, G., & Feuerman, E. (1980). The prevalence of pathogenic and potentially pathogenic fungi on the apparently healthy skin of patients with neoplastic diseases. *Mycopathologia*, 71(2), 85-87.
- Bardaji, D. K. R., da Silva, J. J. M., Bianchi, T. C., de Souza Eugênio, D., de Oliveira, P. F., Leandro, L. F., . . . Tavares, D. C. (2016). Copaifera reticulata oleoresin: chemical characterization and antibacterial properties against oral pathogens. *Anaerobe*, 40, 18-27.
- Bassetti, M., Vena, A., Croxatto, A., Righi, E., & Guery, B. (2018). How to manage Pseudomonas aeruginosa infections. *Drugs in context*, 7.
- Behzadi, P., Baráth, Z., & Gajdács, M. (2021). It's not easy being green: a narrative review on the microbiology, virulence and therapeutic prospects of multidrug-resistant Pseudomonas aeruginosa. *Antibiotics*, 10(1), 42.
- Cianci, P., Slade Jr, J. B., Sato, R. M., & Faulkner, J. (2013). Adjunctive hyperbaric oxygen therapy in the treatment of thermal burns. *Undersea & hyperbaric medicine: journal of the Undersea and Hyperbaric Medical Society, Inc*, 40(1), 89-108.
- Collee, J., Fraser, A., Marmion, B., & Simmons, A. (1996). *Practical medical microbiology*. 14 [sup] th ed. New York: Churchill Livingstone.
- Emmons, S. W. (1974). Bacteriophage lambda derivatives carrying two copies of the cohesive end site. *Journal of molecular biology*, 83(4), 511-525.

- Enders, A. A., North, N. M., Fensore, C. M., Velez-Alvarez, J., & Allen, H. C. (2021). Functional group identification for ftir spectra using image-based machine learning models. *Analytical Chemistry*, 93(28), 9711-9718.
- Feliciano Guzmán, J. M. (2016). Frecuencia y susceptibilidad antifúngica de candida spp aislados en un hospital pediátrico del estado de Chiapas, México. Universidad de Ciencias y Artes de Chiapas,
- Honary, S., Barabadi, H., Gharaei-Fathabad, E., & Naghibi, F. (2012). Green synthesis of copper oxide nanoparticles using *Penicillium aurantiogriseum*, *Penicillium citrinum* and *Penicillium waksmanii*. *Dig J Nanomater Bios*, 7(3), 999-1005.
- Instruments, M. (2012). Dynamic light scattering: an introduction in 30 minutes. Technical Note Malvern, MRK656-01, 1.
- Jalill, A., Raghad, D., Nuaman, R. S., & Abd, A. N. (2016). Biological synthesis of Titanium Dioxide nanoparticles by *Curcuma longa* plant extract and study its biological properties. *World Scientific News*, 49(2), 204-222.
- Jawetz, E., Adelberg, E. A., & Melnick, J. (1987). *Microbiología médica*.
- Jawetz, E., & Melnick, J. (1980). Adelberg. EA. Review of Medical Microbiology, 186-191.
- Jirátová, K., Perekrestov, R., Dvořáková, M., Balabánová, J., Topka, P., Koštejn, M., . . . Kovanda, F. (2019). Cobalt oxide catalysts in the form of thin films prepared by magnetron sputtering on stainless-steel meshes: performance in ethanol oxidation. *Catalysts*, 9(10), 806.
- Li, G., He, D., Qian, Y., Guan, B., Gao, S., Cui, Y., . . . Wang, L. (2012). Fungus-mediated green synthesis of silver nanoparticles using *Aspergillus terreus*. *International journal of molecular sciences*, 13(1), 466-476.
- Maruthamuthu, R., & Ramanathan, K. (2016). Phytochemical analysis of bark extract of *Cinnamomum verum* a medicinal herb used for the treatment of coronary heart disease in malayali tribes. *International Journal of Pharmacognosy and Phytochemical Research*, 8, 1218-1222.
- McGinnis, M. R. (1980). *Laboratory handbook of Medical Mycology*: Elsevier.
- Negi, M., Tsuboi, R., Matsui, T., & Ogawa, H. (1984). Isolation and characterization of proteinase from *Candida albicans*: substrate specificity. *Journal of investigative dermatology*, 83(1), 32-36.
- Pal, S. L., Jana, U., Manna, P. K., Mohanta, G. P., & Manavalan, R. (2011). Nanoparticle: An overview of preparation and characterization. *J Appl Pharm Sci*, 1(6), 228-234.
- Patnaik, P. (2003). *Handbook of inorganic chemicals (Vol. 529)*: McGraw-Hill New York.
- Saad, J. A. A., & Karim, N. F. A. (2017). Evaluation of the antioxidant and inhibitory activity of aloe vera leaf extract

- against some pathogenic bacteria. College of Agriculture, University of Basra, Iraq: Department of Food Sciences,.
- Sokrab, T.-E. O. (2010). See discussions, stats, and author profiles for this publication at: <https://www.researchgate.net/publication/45459776> Hypothalamic hamartoma presenting with gelastic seizures, generalized convulsions, and ictal psychosis.
- Nandagopal P., Steven A.N., Chan L.-W., Rahmat Z., Jamaluddin H., Mohd Noh N.I., 2021. Bioactive Metabolites Produced by Cyanobacteria for Growth Adaptation and Their Pharmacological Properties. *Biology*, 10, 1061. <https://doi.org/10.3390/biology10101061>.
- Nurul Salma Adenan, Fatimah Md. Yusoff and Mohamed Shariff, 2013. Effect of Salinity and Temperature on the Growth of Diatoms and Green Algae. *Journal of Fisheries and Aquatic Science*, 8: 397-404.
- Saeid Aghahosseini Shirazia, Jalal Rastegaryb, Masoud Aghajanic, Abbas Ghassemi, 2018. Simultaneous biomass production and water desalination concentrate treatment by using microalgae. *Desalination and Water Treatment*, 135, pp.101–107.
- Shah, S.M.U., Che Radziah, C., Ibrahim, S., 2014. Effects of photoperiod, salinity, and pH on cell growth and lipid content of *Pavlova lutheri*. *Ann Microbiol*, 64, 157–164. <https://doi.org/10.1007/s13213-013-0645-6>.
- Shaila Hiremath and Pratima Mathad, 2008. Amelioration of Salinity-Induced Metabolic Changes in *Oscillatoria willei* by Gypsum. *J. Algal Biomass Utiln.* 3 (1): 1 – 4.
- Silveira SB., and Odebrecht C., 2019. Effects of Salinity and Temperature on the Growth, Toxin Production, and Akinete Germination of the Cyanobacterium *Nodularia spumigena*. *Front. Mar. Sci.* 6:339. doi: 10.3389/fmars.2019.00339
- Suryasa, I. W., Rodríguez-Gámez, M., & Koldoris, T. (2021). Health and treatment of diabetes mellitus. *International Journal of Health Sciences*, 5(1), i-v. <https://doi.org/10.53730/ijhs.v5n1.2864>
- Valipour A., Hamnabard N., Woo K.S., Ahn Y.H., 2014. Performance of high-rate constructed phytoremediation process with attached growth for domestic wastewater treatment: Effect of high TDS and Cu. *J. Environ. Manag.*, 145, 108.
- Wangwibulkit Somchai, Limsuwan Chalor, and Chuchird Niti, 2008. Effects of Salinity and pH on the Growth of Blue-Green Algae, *Oscillatoria* sp. and *Microcystis* sp., Isolated from Pacific White Shrimp (*Litopenaeus vannamei*) Ponds. *Journal of fisheries and environment*, Vol. 32 No. 1.